Supporting Information for

Fewer-layer conductive metal-organic nanosheets enable ultrahigh mass activity for the oxygen evolution reaction†

Mingdao Zhang,[a]* Bao-Hui Zheng,[b] Jing Xu,[a] Na Pan,[a] Jianghua Yu,[a]* Mindong Chen,[a] and Hui Cao[a]*

---

[a] *Department of Chemistry, Jiangsu Key Laboratory of Atmospheric Environment Monitoring and Pollution Control, School of Environmental Science and Engineering, Nanjing University of Information Science & Technology, Nanjing 210044, Jiangsu, P. R. China. E-mail: matchlessjimmy@163.com; yujhnuist@163.com; yccaoh@hotmail.com.*

[b] *Institute of Chemical Materials, Chinese Academy of Engineering Physics, Mianyang 621999, Sichuan, P. R. China. E-mail: zhengbaohui305@126.com.*

Experimental

1. **Materials and measurements**

All chemicals and reagents were commercially available and used as purchased without further purification.

IR absorption spectra of the complexes were recorded in the range of 400–4000 cm^{-1} on a Nicolet (Impact 410) spectrometer. X-ray photoelectron spectroscopy (XPS) measurements were carried out on a PHI-5300 ESCA spectrometer (PerkinElmer) using 300W Al Kα radiation. The corresponded binding energies were referenced to the C 1s line at 284.8 eV from adventitious carbon. Ultraviolet-visible (*UV-vis*) spectroscopy was investigated with a Shimadzu UV-3600 using a 10 mm quartz cuvette that dissolves the ligands. The morphology and nanosheet thickness of HTM nanosheets were investigated by atomic force microscopy (AFM) using Agilent 5500 AFM. Infrared spectra were recorded on a Nicolet FT-IR 730 with an ATR unit (Zn-Se crystal). The water contact angles were measured on a contact angle measurement system (OCA 30, Data Physics Instruments GmbH). Scanning electron microscopic (SEM) images were taken on a Nova Nano SEM 600.

2 Langmuir-Blodgett experiments and transferring the metal-HHTP single-layers on to the substrates

Nanosheets were prepared on a Langmuir-Blodgett trough using Millipore water and placed on an anti-vibration table according to a procedure developed in reference.[S1, S2]

The typical experiment for mono-metal based LB nanosheets was performed as follows: Firstly, 10 μL of a 0.5 mM stock solution of HHTP in DMF/chloroform (v/v=1:3) was dispersed on the water surface. The solvent was allowed to evaporate for 30 minutes, and compression was then performed at a rate of 2 mm min^{-1}. When the surface pressure reached -1.0 mN m^{-1} (relative to pure water, Fig. S4), 4 mL of a freshly prepared metal salt solution of 5 mM $Co(OAc)_2$ + 1 mM NaOAc was injected into the water phase with a syringe to reach a final salt concentration of ~ 1.0 mM. This concentration represents an approximately 1000-fold excess of metal salt relative to the monomer concentration. Two hours later, the thus formed nanosheet was horizontally transferred onto an FTO glass. Subsequently, the sample was rinsed with water and then dried at room temperature.

3 Electrochemical characterizations

The electrocatalytic performance of the LB nanosheets for oxygen evolution reactions (OER) was investigated with a three-electrode cell[S3] on CHI760E electrochemical workstation. A Pt foil (1 cm^2) was used as the counter electrode for OER test, respectively. Saturated calomel electrode (SCE) was selected as the reference electrode. The catalytic performance for OER was measured from 1.0 to 1.9 V vs. RHE in 0.1 M O_2-saturated KOH electrolyte.

During the evaluations of OER performances of the $[Co_3(HHTP)_2]_n$ LB nanosheets and RuO_2, the FTO glasses loading the $[Co_3(HHTP)_2]_n$ LB nanosheets were used as the working electrodes directly, while the RuO_2, hardly to be made as fewer-layer nanosheets, was loaded to a RDE (rotating disk electrode, 5 mm in diameter).

The RuO_2 working electrode was prepared as follows: 2 mg of catalyst was added into 0.4 mL of ethanol and 40 μL of 5 wt% perfluorosulfonic acid (PFSA), which was dispersed by ultrasonication for approximately 30 min to obtain a homogeneous suspension. Next, 10 μL of the dispersion was uniformly dropped onto the RDE and was dried under ambient conditions. The resulted loading density of RuO_2 on the RDE was 0.255 mg/cm^2.

All of the electrochemical tests were performed at room temperature of *ca.* 25 °C. All of the potentials and voltages are iR corrected, and calibrated and converted to reversible hydrogen electrode.[S4] All electrochemical experiments were performed at 25 ± 1 ºC.

4 UV-vis spectroscopy characterizations

UV-vis spectroscopy was utilized to characterize the as-prepared LB nanosheets. As shown in Fig. S7a, the HHTP solution showed intense absorption from 250 to 300 nm, which can be attributed to the inter-molecular π-π* interactions of HHTP.

The UV-vis absorption intensities of HHTP solutions with different concentrations at 281 nm (Fig. S7a) respected to a linear trend (Fig. S7b).[S5] The equation of the absorption intensity, HHTP concentration, and layer number is:

$$y = 0.0878x + 0.0387 = 0.00917n + 0.0387 \tag{1}$$

in which y is the absorption intensity, and x represents the concentration of HHTP. Additionally, n is the layer number, which is calculated from the hole diameter of the metal-organic structure (Fig. 1a) with an area HHTP concentration of $7.83*10^{-11}$ mol/cm^2.

HHTP molecules in the 3-layer $[Co_3(HHTP)_2]_n$ LB nanosheets were further dissolved, and the solutions' UV-vis absorption patterns are shown in Fig. S8. Meanwhile, the maximum absorption intensities indicate the layer numbers 3-layer $[Co_3(HHTP)_2]_n$ LB films as 2.97, demonstrating that single-layer LB nanosheet can be dipped no matter onto the FTO substrate or LB nanosheets every time.

5 First-principles calculations using density functional theory (DFT)

Density functional calculations were performed using the Gaussian09 package at the basis level of 6-31G(d) for C, H, and O atoms and Lanl2DZ for Co atom with the B3LYP functional. The edge carbon atoms in the small fragment of the $[Co_3(HHTP)_2]_n$ nanosheet was saturated with hydrogen atoms.

5 Additional Figures for metal-organic $[Co_3(HHTP)_2]_n$ LB nanosheets

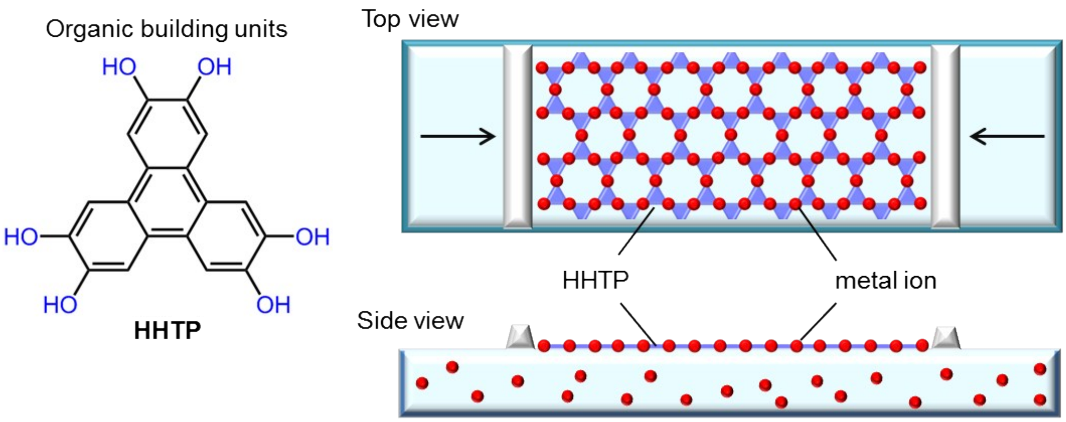

Fig. S1. Schematic illustration of the representative assembly processes of $[Co_3(HHTP)_2]_n$ LB nanosheets.

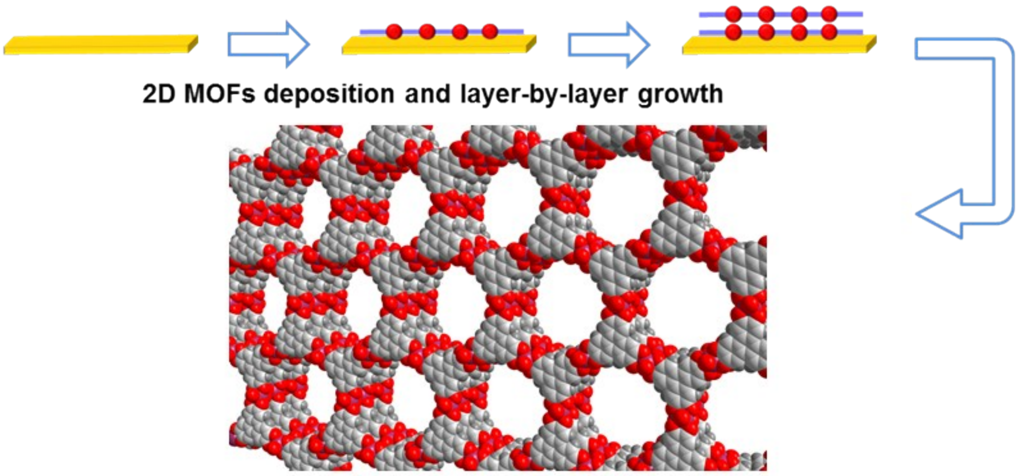

Fig. S2. The combined Langmuir-Blodgett/layer-by-layer (LB-LbL) nanofilms growth technique.

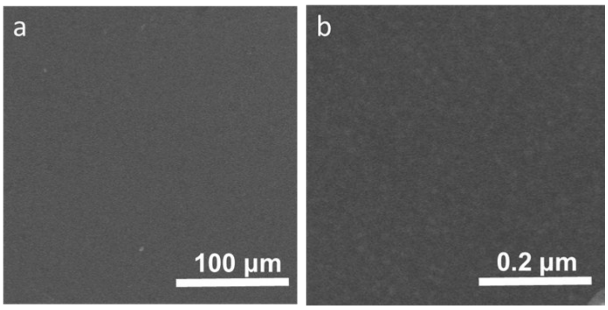

Fig. S3. SEM images of 4-layer $[Co_3(HHTP)_2]_n$ nanosheets.

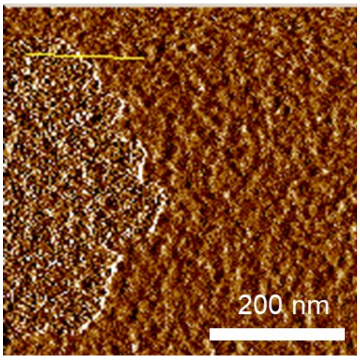

Fig. S4. AFM amptitude image of single-layer $[Co_3(HHTP)_2]_n$ nanosheet.

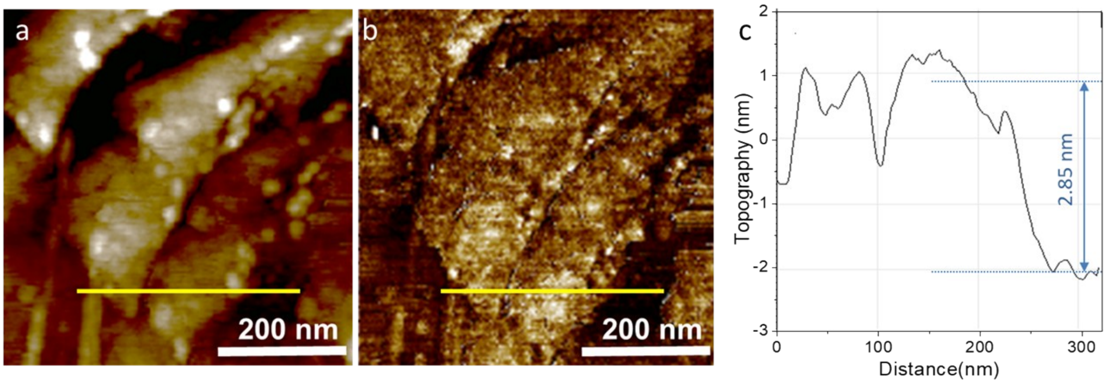

Fig. S5. (a) AFM topography image of 4-layer $[Co_3(HHTP)_2]_n$ LB nanosheets; (b) AFM phase image of 4-layer $[Co_3(HHTP)_2]_n$ LB nanosheets; (c) Corresponding line profiles of the yellow line in Figs. S4a and S4b.

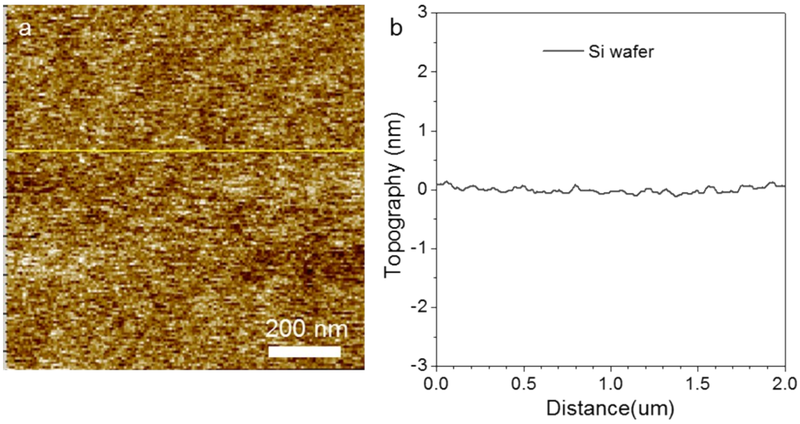

Fig. S6. (a) AFM topography image of Si wafer; (b) Corresponding line profiles of the yellow line in S4a.

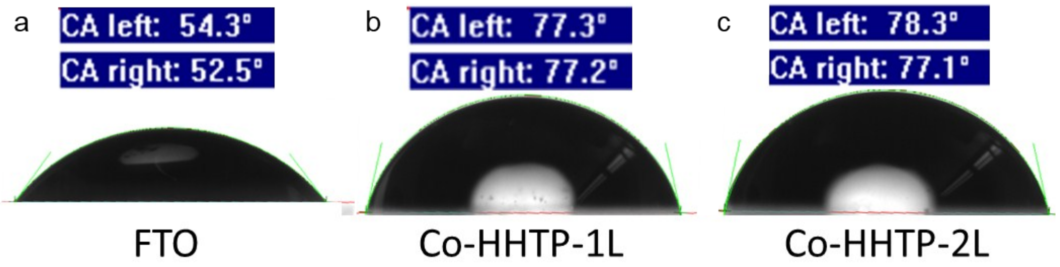

Fig. S7. Water contact angles of (a) FTO glass, (b) single-layer $[Co_3(HHTP)_2]_n$ LB nanosheet, and (c) double-layer $[Co_3(HHTP)_2]_n$ LB nanosheets.

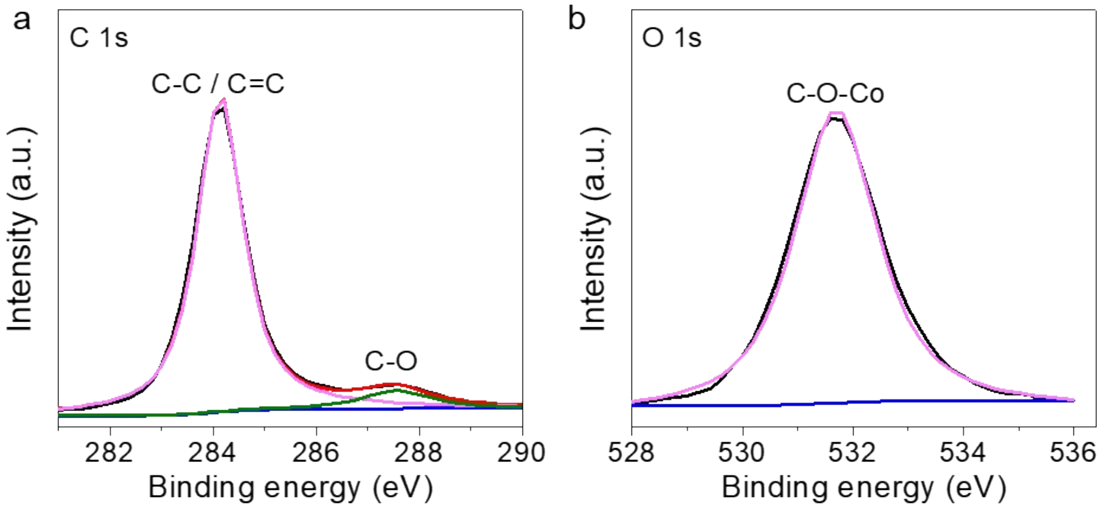

Fig. S8. (a) C 1s and (b) O 1s spectra of $[Co_3(HHTP)_2]_n$ LB nanosheets.

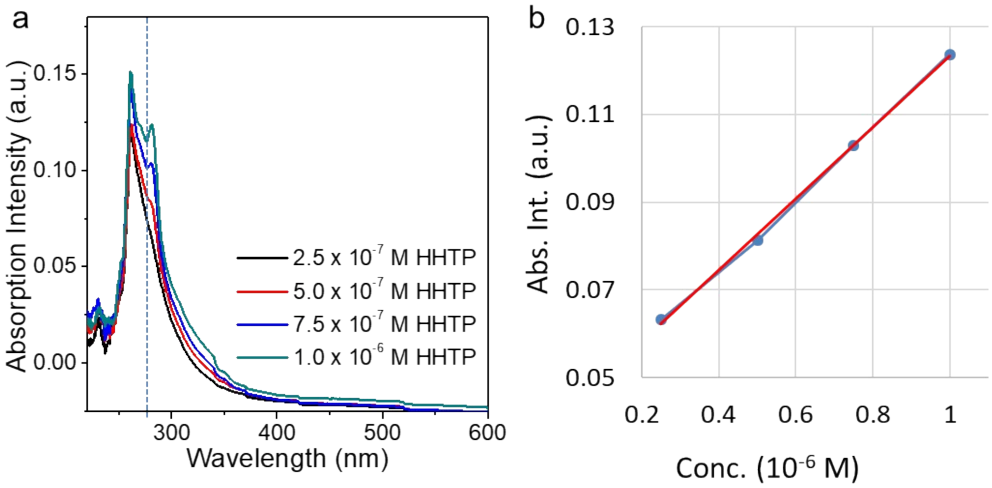

Fig. S9. (a) UV-vis absorption spectra of HHTP solution at different concentrations; (b) The linear relationship between the absorbance at 282 nm and the concentration.

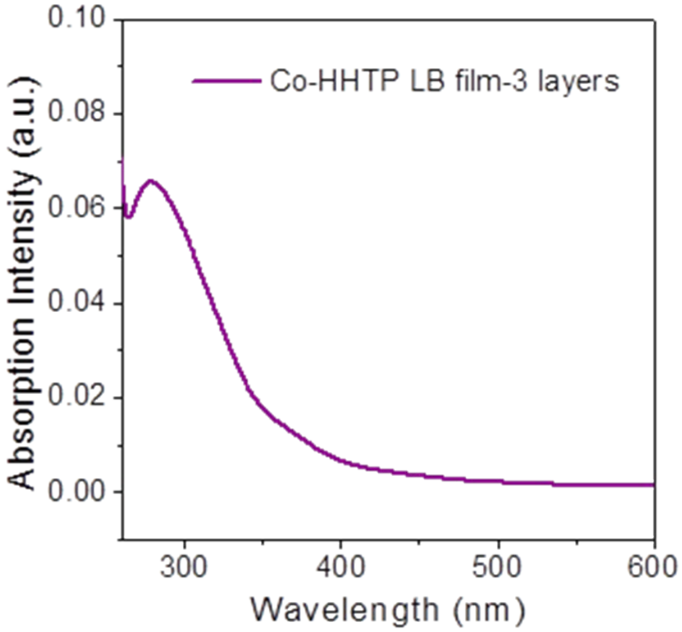

Fig. S10. UV-vis absorption spectra of $[Co_3(HHTP)_2]_n$ LB 3-layer nanosheets

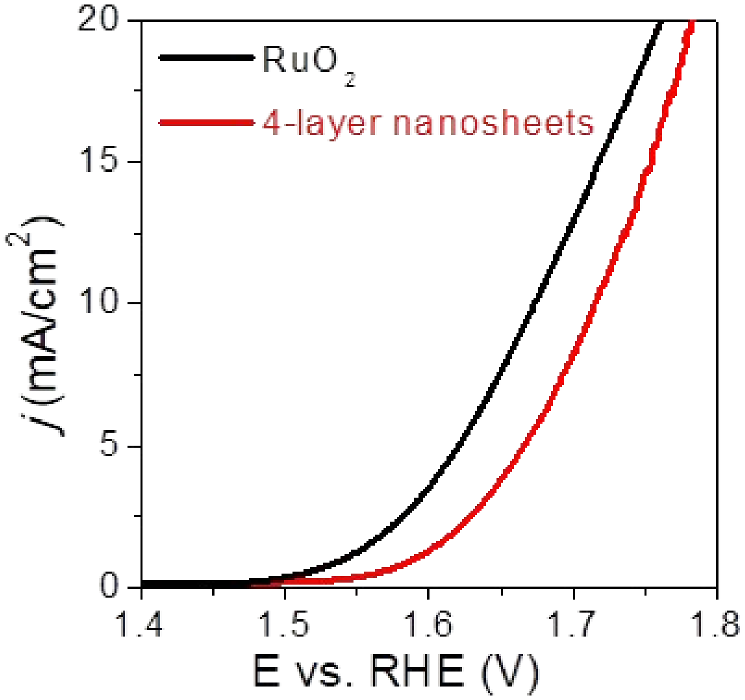

Fig. S11. LSV curves of 4-layer $[Co_3(HHTP)_2]_n$ LB nanosheets and RuO_2 to the extent of the unit area.

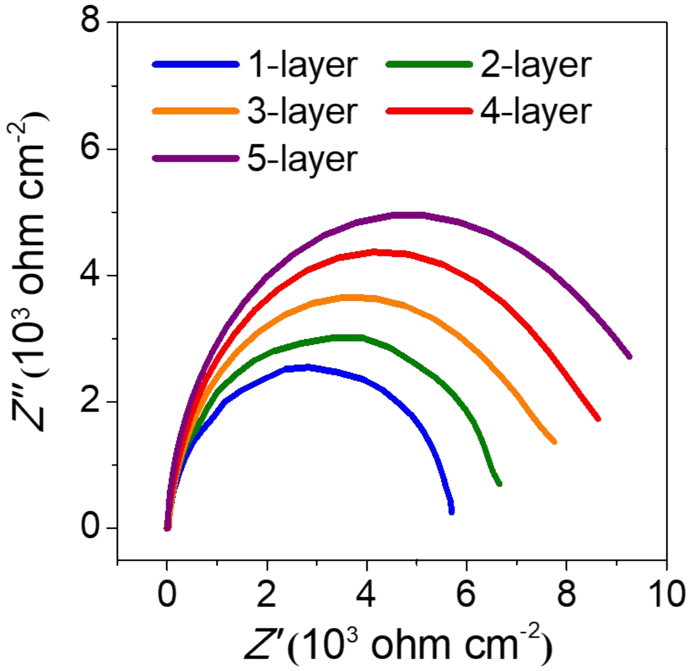

Fig. S12. Electrochemical impedance spectra (EIS) of 1,2,3,4,5-layer $[Co_3(HHTP)_2]_n$ LB films.

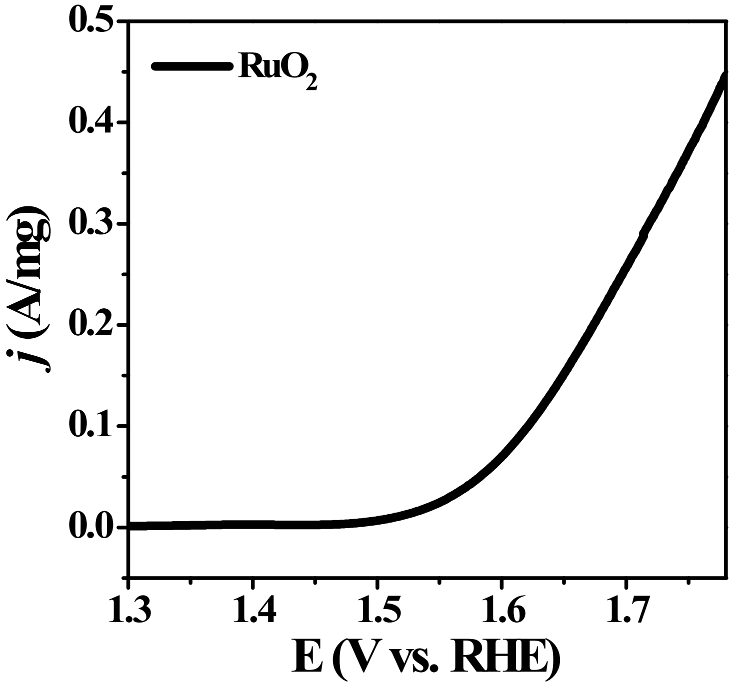

Fig. S13. Enlarged LSV curves of RuO_2 to the extent of unit weight.

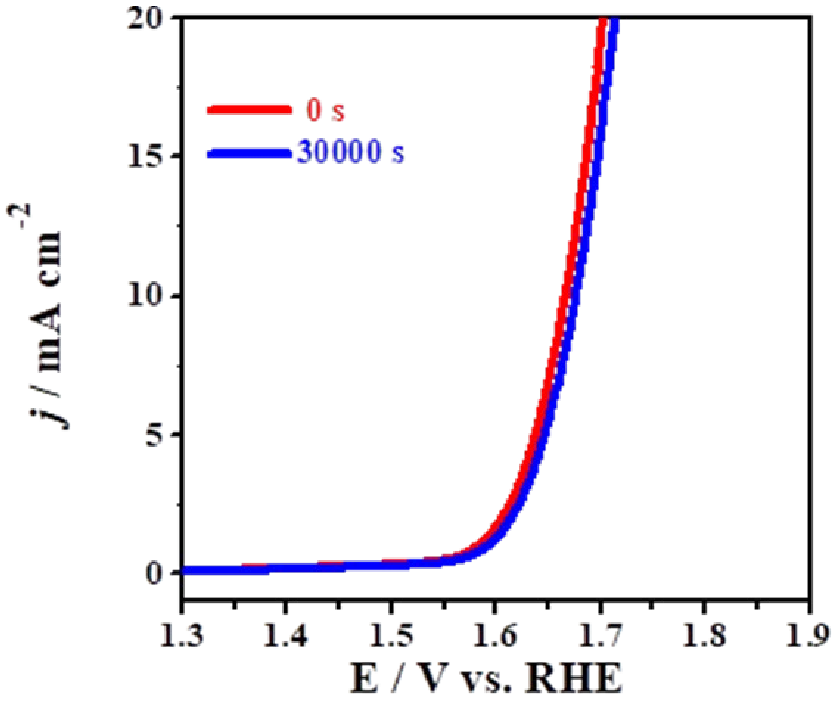

Fig. S14. LSV plots before and after durability evolution for OER of $[Co_3(HHTP)_2]_n$ LB nanosheets.

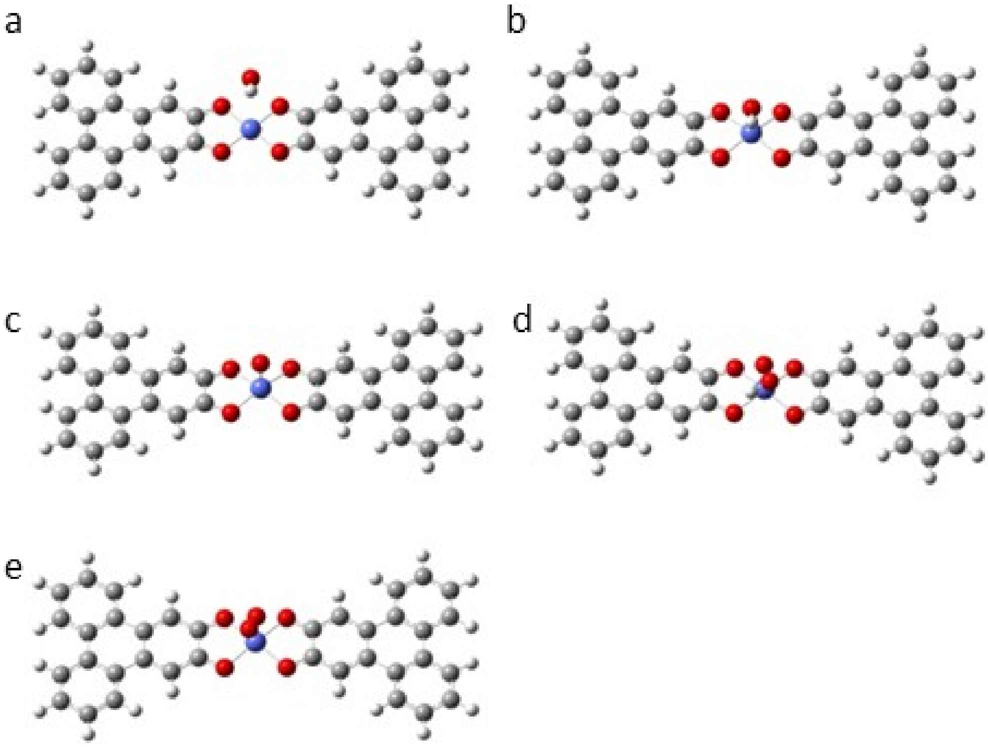

Fig. S15. (a-e) Initial structure (a) and structures after the adsorption of one electron (b), two electrons (c), three electrons (d), four electrons (e).

References

S1 Z. Zheng, L. Opilik, F. Schiffmann, W. Liu, G. Bergamini, P. Ceroni, L. Lee, A. Schütz, J. Sakamoto, R. Zenobi, J. VandeVondele, A. D. Schlüter, *J. Am. Chem. Soc.*, **2014**, *136*, 6103.

S2 R. Makiura, O. Konovalov, *Sci. Rep.*, **2013**, *3*, 2506.

S3 Y. Yang, H. Fei, G. Ruan, J. M. Tour, *Adv. Mater.*, **2015**, *27*, 3175-3180.

S4 W. Sheng, H. A. Gasteiger, Y. Shao-Horn, *J. Electrochem. Soc.*, **2010**, *157*, B1529-B1536.

S5 H. R. Gordon, *Limnol. Oceanogr.*, 1989, **34**, 1389-1409.